Huang *et al. Human Genomics* (2026) 20:72
https://doi.org/10.1186/s40246-026-00945-8

Human Genomics

RESEARCH Open Access

Leveraging proteomics and machine learning for mechanism and biomarker discovery on glioma progression and transformation: from LGG to GBM

Qinhong Huang[1†], Hui Liang[1†], Jie Liu[1†], Shenbao Shi[1], Xinlin Sun[1], Yiquan Ke[1,2*] and Taoliang Chen[1*]

Abstract

Background Glioma was the most common malignant tumor of the central nervous system in adults. Low-grade gliomas (LGGs) have a potential of grade progression and histological transformation, and the relevant mechanisms of this malignant evolution were still unclear.

Methods In this study, we used 61 primary-recurrent paired glioma samples from 28 patients for proteomics analysis based upon DIA-NN approach.

Results Our results indicated that the Ras/p38-MAPK pathways were hub signaling pathways driving grade progression and histological transformation in LGG. The activation of non-MGMT dependent unspecific DNA damage repair system mediated by Replication Factor C (RFC) can be an important reason for the treatment resistance. Moreover, metabolic reprogramming was widely involved in the regulation of LGG grade progression and histological transformation. The enhanced synthesis of unsaturated fatty acids and the significantly activated peroxisomal fatty acid beta-oxidation pathways were metabolic characteristics of LGG after histological transformation. Last, we constructed a reliable LGG progression prediction model consisted of 2 proteins, which can be monitor biomarkers for LGG progression, with potential clinical translation value.

Conclusions In summary, glioma grade progression and histological transformation were complex biological processes, which involved the abnormal up-regulation of Ras/p38-MAPK signalings, enhanced non-MGMT dependent unspecific DNA damage repair system regulated by RFC complex and metabolic reprogramming based on HK1-PFKP-ENO2 mediated glycolysis and peroxisomal FA beta oxidation. This study filled the gap in relevant research on the grade progression and histological transformation of LGG, providing novel and unique insights into the biological mechanisms of glioma progression.

†Qinhong Huang, Hui Liang and Jie Liu are first authors.

*Correspondence:
Yiquan Ke
kyquan@smu.edu.cn
Taoliang Chen
1073758862@qq.com

Full list of author information is available at the end of the article

Importance of the study

- As far as we know, this is the first study to uncover the potential biological mechanisms of glioma grade progression and histological transformation at proteomics level through paired primary-recurrent glioma samples. We revealed that glioma grade progression and histological transformation were complex biological processes, involving abnormal up-regulation of MAPK cascade pathways, enhancing non-MGMT dependent unspecific DNA damage repair system and metabolic reprogramming. Besides, PGM2L1 and ZNF24 were identified as LGG progression biomarkers with high prediction efficacy.

Keywords Proteomics, LGG, Grade progression, Histological transformation, Metabolic reprogramming

Graphical Abstract

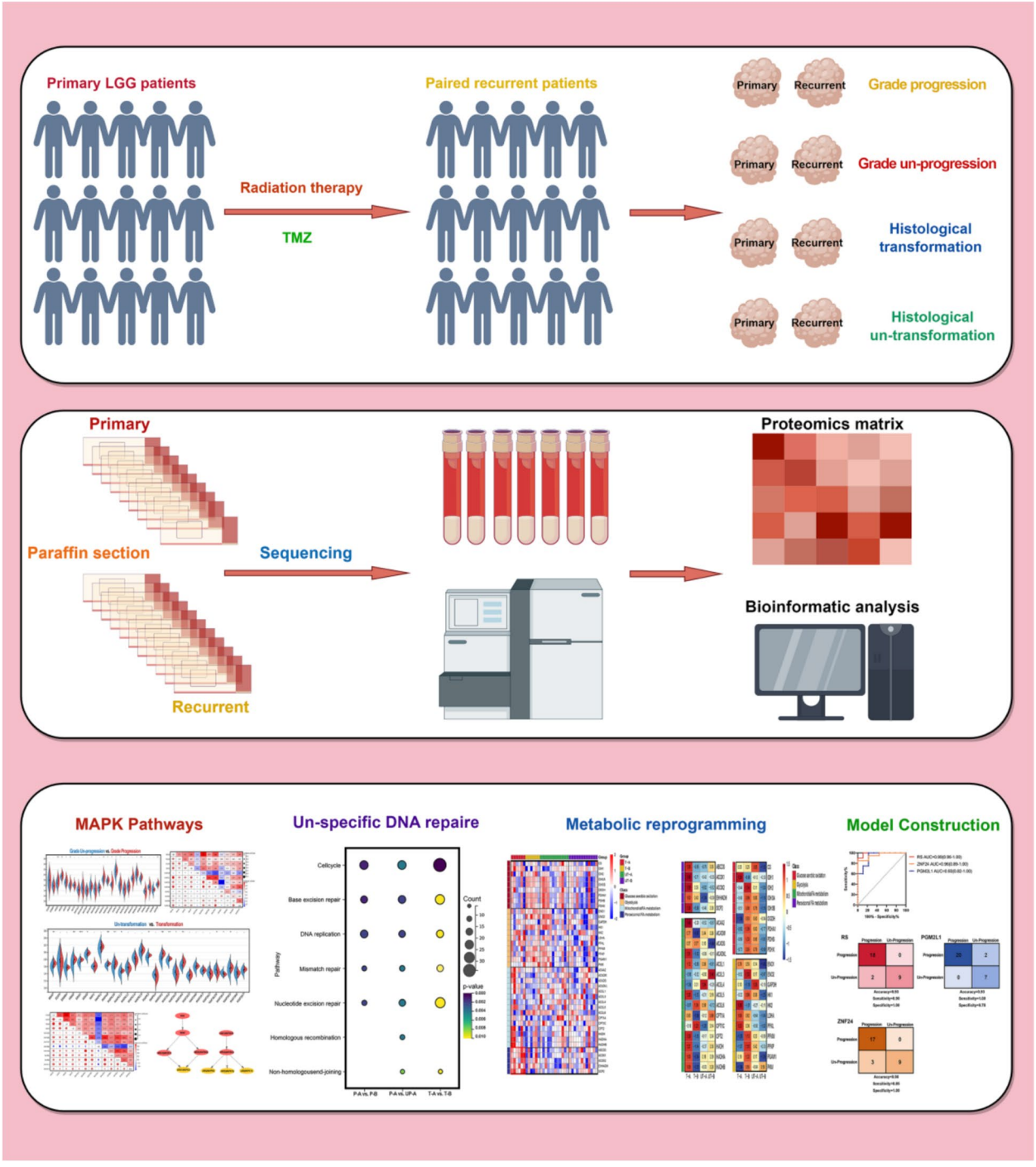

Introduction

Gliomas were the most common primary malignant tumors of the central nervous system, with high mortality and recurrence rates [1]. Among them, WHO grade II–III gliomas were considered as LGG, mainly composed of IDH mutant oligodendrogliomas and astrocytes. WHO grade IV glioma was mainly composed of glioblastoma, which was the most malignant glioma, with a median survival time of only 14.9 months [2]. Currently, the primary treatment option for gliomas was surgery combined with oral temozolomide (TMZ) and radiation therapy [3]. The roles of TMZ and radiation therapy were non-selective DNA damage, and under this treatment, almost all patients will suffer from recurrence, with recurrent tumors carrying significant alterations that may result in drug resistance [4]. In addition, in clinical practice, it has been found that many LGG patients suffered from WHO grade progression and histological transformation during recurrence, accelerating the progression of the disease [5]. Therefore, there was an urgent need to discover and elucidate the biological mechanisms of LGG grade progression and histological transformation to guide the development of new treatment strategies.

At present, a limited number of articles have explored the mechanisms of LGG to GBM progression, and found the roles of PI3K/Akt/mTOR pathway, RB pathway [6, 7], cell cycle regulation [8], DNA methylation reprogramming [9], and MET-exon-14-skipping (METex14) [10] in LGG progression. But these efforts mainly focused on genomics, transcriptomics, and epigenetics. Meanwhile, most previous omics studies compared tumors across WHO grades but rarely analyzed paired primary-recurrent gliomas. Lacking in-depth studies on how LGG underwent grade progression and histological transformation at the proteomics level using paired primary-recurrent glioma samples. It was worth noticing that many multi-omics studies have reported a low correlation between mRNA and protein expressions, indicating that inferring proteins expression solely based on studying mRNA-sequencing was limited [11–13]. Proteomics provided another paradigm for studying the hidden dimensions of cancer biology, which were largely undiscovered.

Therefore, this study collected paired primary-recurrent samples of 28 glioma patients for proteomics analysis, revealing the potential biological mechanisms of LGG grade progression and histological transformation at the protein level. This study provided a novel and unique insight into the biological mechanisms of LGG grade progression and histological transformation at the protein level, opening up new avenues for future research.

Results

Research overview

Cohorts characteristics

In order to explore the potential biological mechanisms of LGG grade progression and histological transformation, we retrieved the glioma patients in the Zhujiang Hospital, and finally collected a total of 61 glioma samples to consist Zhujiang cohort. In the cohort, there were 17 paired primary-recurrent LGG samples with grade progression and/or histological transformation at the time of recurrence. Among these patients, 3 patients had recurred twice with grade progression each time. In addition, there were 8 patients who maintained their original grade and histological types at the time of recurrence. Among them, 1 patient had recurred twice and maintained the same grade and histological type as the primary tumor. 3 paired primary-recurrent glioblastoma samples were also collected for analysis (Supplemental Table S1). It is worth noting that the primary histological types of patients who experienced histological transformation all contained oligodendrocyte components (6 cases of oligodendroglioma), and no cases of transformation from astrocytoma to oligodendroglioma have been collected yet. We excluded astrocytoma to glioblastoma progression from histological transformation, because glioblastoma was generally believed to be astrocytic histology [14]. All patients did not receive any treatment before the first glioma resection surgery. All patients received oral TMZ combined with radiation therapy after surgery. Additionally, we collected clinical data from all glioma patients in the TCGA database, CGGA mRNA-seq_693 dataset, and CGGA mRNAseq_325 dataset for survival analysis.

Proteomics-sequencing quality and research significance

We conducted qualitative and quantitative proteomics-sequencing on all 61 glioma samples. The proteomics-sequencing of all the samples were conducted in one batch, so there was no significant batch effect. The length distribution of the peptide segments identified by mass spectrometry met the quality control requirements (Supplemental Figure S1A-B). The protein abundance converted by Log2 and standardized were highly comparable among the 61 samples in the entire cohort (Supplemental Figure S1C). A total of 8067 proteins were identified in at least 75% of the samples for subsequent analysis.

Survival analysis of clinical data from all integrated cohorts of glioma patients demonstrated significant different prognosis among oligodendroglioma, astrocytoma and glioblastoma patients. The prognosis of oligodendroglioma patients was the best among the four histological types, the prognosis of mixed glioma patients was between oligodendroglioma patients and astrocytes, and glioblastoma patients had the worst prognosis. In

addition to histological types, gliomas with different WHO grades have varying impacts on prognosis, with higher grades resulting in poorer outcomes (Supplemental Figure S1D-E). The integrated proteomics analysis of 61 samples reported significant differences in protein expression pattern among oligodendroglioma that underwent histological transformation (OT), oligodendroglioma (O), astrocytoma (A) and glioblastoma (G) (Supplemental Figure S1F). Therefore, exploring the biological mechanisms of glioma progression through proteomics was a feasible strategy.

Potential mechanism of WHO grade progression of LGG

The up-regulation of key proteins in the MAPK cascade signaling pathways drove LGG grade progression

In clinical practice, it is inevitable that some LGG patients suffered from recurrence accompanied by grade progression, which had a catastrophic impact on their prognosis. Aiming to explore the potential mechanism of LGG grade progression, we conducted GSEA analysis and ssGSEA in the primary LGG, and consistently found that the "MAPK pathway" was significantly enriched in the grade progression group ($|NES| > 1$, $p < 0.05$, $FDR < 0.25$) (Supplemental Figure S2A, B). In view of the multiple branch pathways in MAPK pathways, we examined the expression levels of key proteins and found that the key proteins of 2 complete cascade signaling pathways were consistently over-expressed in grade progression group, which were Ras-BRAF-MEK1/2-ERK1/2 and ASK1-MEK4-JNK2/3, respectively (Fig. 1A). The expression levels of these key proteins demonstrated significantly strong positive correlations, revealing the close interactions among them (Fig. 1B, C).

Further, we conducted differential expressed protein (DEP) analysis on two primary glioma groups (grade progression before: P-B; grade un-progression before: UP-B). As a result, 1275 DEPs (16%) were identified between the two groups, with 500 proteins significantly over-expressed in the P-B group (Supplemental Table S4). Functional enrichment analysis of the 500 proteins revealed that these proteins were widely involved in various phosphorylation processes, affecting cellular signal transduction (Supplemental Table S5). More importantly, these proteins were not only enriched in the MAPK pathways mentioned above, but also significantly enriched in the downstream mTOR-HIF1a-metabolic pathways (Supplemental Figure S2C). Among these pathways, we noticed that the proteins involved in HIF-1a and its downstream pathways, such as carbon metabolism, glycolysis, and pyruvate metabolism, were significantly up-regulated in the P-B group (Supplemental Table S6). To further determine the up-regulation of the downstream glycolysis pathway, we compared the key enzymes of glycolysis between P-B and UP-B groups. The results demonstrated that the vast majority key enzymes of glycolysis were significantly up-regulated in the P-B group, including ENO1, ENO2, HK1, LDHA, PFKP, PFKM, PGAM1 and PKM, indicating that the enhanced glycolysis process in P-B group (Fig. 1D). However, HK2, previously shown to up-regulated in various cancers [15, 16], did not found significant expression difference between the two groups in our analysis. The correlation analysis between enzymes uncovered that the glycolysis process driven by HK1-PFKP-ENO2 was significantly activated in the P-B group (Fig. 1E). Based on this, we speculated that the activation of MAPK and its downstream pathways resulted in "sugar metabolism reprogramming" dominated by enhanced glycolysis, which provided energy and drove LGG grade progression.

In order to verify the up-regulation of the MAPK pathways in the primary LGG has potential driving effect on grade progression, we divided P-B group into 2 subgroups: grade-by-grade progression group (Grade 2 to 3 / Grade 3 to 4) and cross grade progression group (Grade 2 to 4), and then evaluated the expression levels of proteins involved in the above pathways (Fig. 1F). The results demonstrated that the above up-regulated pathways in P-B group were further up-regulated in cross grade progression group (Fig. 1G). Moreover, HK1, PFKP and ENO2 were further up-regulated, emphasizing that these three glycolytic enzymes played important roles in regulating the glycolysis process (Fig. 1H-I). Among these three glycolytic enzymes, HK1, as the rate limiting enzyme in the first step of glycolysis, was the key regulator of the entire glycolysis metabolism process. Our result found that HK1 participates in various glucose metabolism related pathways involved in LGG grade progression (Supplemental Figure S2D), which indicated that the abnormal expression of HK1 may be the core regulatory factor of "sugar metabolism reprogramming" in P-B group, having potential targeted significance.

Enhanced Non-MGMT dependent unspecific DNA damage repair contributed to therapy resistance and grade progression

To investigate the differences between LGG before and after grade progression (P-B vs. P-A), we conducted DEP analysis and functional annotation. 946 DEPs (12%) were identified between P-B and P-A group, and 571 DEGs were significantly up-regulated in the P-A group (Supplemental Figure S3A) (Supplemental Table S4). Functional analysis of these 571 up-regulated proteins demonstrated that most of them were binding proteins of chromatin, DNA, RNA and protein, participating in chromatin remodeling, DNA replication, transcription, and translation processes, which indicated more active cell proliferation and division behaviors in P-A group (Supplemental Table S5). Pathway enrichment analysis

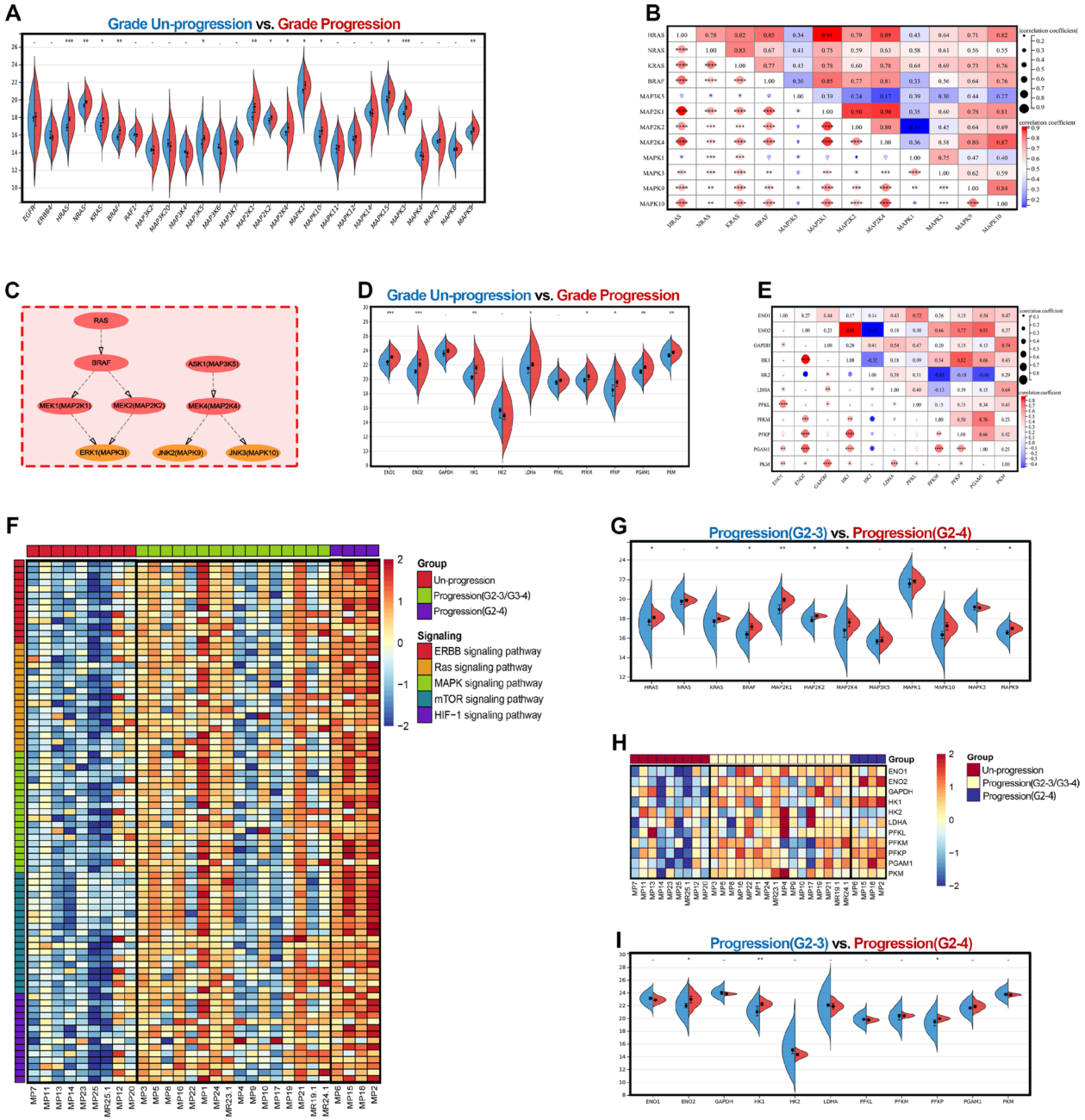

Fig. 1 Up-regulated MAPK pathways and glycolysis in P-B group. **A** Different expression levels of key protein kinases in MAPK pathways between P-B and UP-B groups; **B** Correlations of over-expressed key protein kinases in MAPK pathways in P-B group; **C** Tow up-regulated MAPK cascade pathways in P-B group; **D** Different expression levels of key enzymes in glycolysis between P-B and UP-B groups; **E** Correlations of key enzymes in glycolysis in P-B group; **F** Heatmap revealing different expression levels of proteins involved in MAPK related pathways among grade un-progression group, grade-by-grade progression group and cross grade progression group; **G** Different expression levels of over-expressed key protein kinases in MAPK pathways between grade-by-grade progression group and cross grade progression group; **H** Heatmap revealing different expression levels of key enzymes in glycolysis among grade un-progression group, grade-by-grade progression group and cross grade progression group; **I** Different expression levels of key enzymes in glycolysis between grade-by-grade progression group and cross grade progression group

revealed that these up-regulated proteins were widely involved in processes such as cell cycle, base excision repair, mismatch repair and nucleotide excision repair, suggesting the stronger therapy resistance characteristic of P-A group (Supplemental Table S6). It was worth noting that all of our patients received TMZ and radiotherapy. TMZ, as an alkylating agent, has cytotoxicity mainly towards DNA methylation, occurring at the N7 and O6 positions of guanine [17]. Base excision repair, mismatch repair, and nucleotide excision repair can

highly match and counteract the cytotoxic effects of TMZ. In addition, base excision repair and nucleotide excision repair also played key roles in repairing DNA damage caused by radiotherapy.

To further examine that the enhanced DNA replication and damage repair pathways were closely related to the LGG grade progression, we divided all recurrent LGG samples into two groups based on grade progression or not (grade progression after: P-A; grade un-progression after: UP-A). The results showed that there were 1146 (14%) DEPs between P-A and UP-A group, among which, 865 proteins were significantly over-expressed in the P-A group (Supplemental Figure S3B)(Supplemental Table S4). Functional enrichment analysis revealed that, consistent with the above, most of the over-expressed proteins in the P-A group were binding proteins of chromatin, DNA, RNA and protein, participating in chromatin remodeling, DNA replication, transcription, and translation processes. Pathway enrichment analysis further demonstrated that the above-mentioned DNA replication and repair pathways were also significantly enriched in the P-A group (Supplemental Figure S3C) (Supplemental Table S5-6). From these, we can basically speculate that the up-regulation of unspecific DNA damage repair pathways contributed to the LGG grade progression by enhancing therapy resistance.

Due to the fact that all of our patients received TMZ treatment and the cytotoxic effect of TMZ can be reversed by MGMT [17, 18], we evaluated the MGMT level among 4 groups: grade progression before and after, grade un-progression before and after (P-B, P-A, UP-B, UP-A) to investigate whether the enhanced therapy resistance characteristic depends on MGMT expression. Results reported no significant difference in the MGMT expression level among 4 groups (Supplemental Figure S3D-E). Therefore, the TMZ resistance mechanism in the P-A group may not rely on MGMT, but more on self-repair systems such as base excitation repair, mismatch repair, and nucleotide excitation repair. They can not only reverse the damage of TMZ, but also resist radiation damage, which can explain why MGMT methylated patients still suffered from recurrence after TMZ therapy and recurrent gliomas were generally TMZ useless.

Nevertheless, by analyzing the DNA replication and repair pathways, we found that RFC5, RFC3, RFC4, PCNA, RFC2, and POLD2 were hub proteins, which persistently over-expressed in P-A groups when compared to either P-B group or UP-A group. Among them, RFC5, RFC3, RFC4 and RFC2 were parts of RFC, and can directly interacted with PCNA, regulating DNA replication and damage repair (Supplemental Figure S3F-K) [19–24]. Therefore, this result suggested that RFC can be the key regulator of DNA replication and damage repair system in LGG grade progression.

The relationship between glycolysis and non-MGMT dependent unspecific DNA damage repair

Previous studies have shown a close relationship between glycolysis and DNA damage repair, and the over-expression of various glycolytic enzymes can significantly enhance DNA damage repair ability. However, in the exploration of the relationship between glycolysis level and DNA damage repair ability, we found two interesting results. The first one was that in the comparison between UP-A and UP-B groups, we observed that most glycolytic enzymes were significantly over-expressed in the UP-A group, including HK1, PFKP and ENO2, except HK2 (Fig. 2A). However, surprisingly, in the comparison between P-A and P-B groups, most of the glycolytic enzymes were down-regulated in P-A group, with increase in HK2 and no significant change in LDHA (Fig. 2B). Combining with the above analysis, this result indicated the enhanced glycolysis in primary LGG could promote grade progression during recurrent, but after recurrent, complex metabolic reprogramming appeared.

The other interesting result was that when extended our analysis into all the paired LGG samples, we found that the stronger glycolysis process driven by HK1 the primary samples had, the stronger the DNA damage repair ability the recurrent samples had. Results demonstrated that the expression level of the above hub DNA damage repair proteins in recurrent group were significantly negatively correlated with the expression of glycolytic enzymes in recurrent group, including HK1, PFKP and ENO2; while they were significantly positively correlated with the expression of glycolytic enzymes in primary group (Fig. 2C, D).

Potential biological mechanisms of oligodendroglioma histological transformation

The up-regulated MAPK cascade pathways may drive oligodendroglioma histological transformation

In our Zhujiang cohort, we found that a part of LGGs suffered from histological transformation when they recurred, and only occurred in oligodendroma or oligoastrocytoma. To investigate the potential biological mechanisms of oligodendroglioma histological transformation, we first divided all the primary oligodendroglioma (including oligoastrocytoma in all the subsequent analysis) into two groups based on whether histological transformation or not (transformation before: T-B; un-transformation before: UT-B), and explored the differences in proteomics between the two groups. DEP analysis demonstrated that 2997 (37%) proteins exhibited significant differential expression between the two groups, with only about 784 proteins over-expressed in T-B group (Supplemental Table S4). Functional enrichment analysis reported that the 784 proteins over-expressed in T-B group were mainly binding proteins

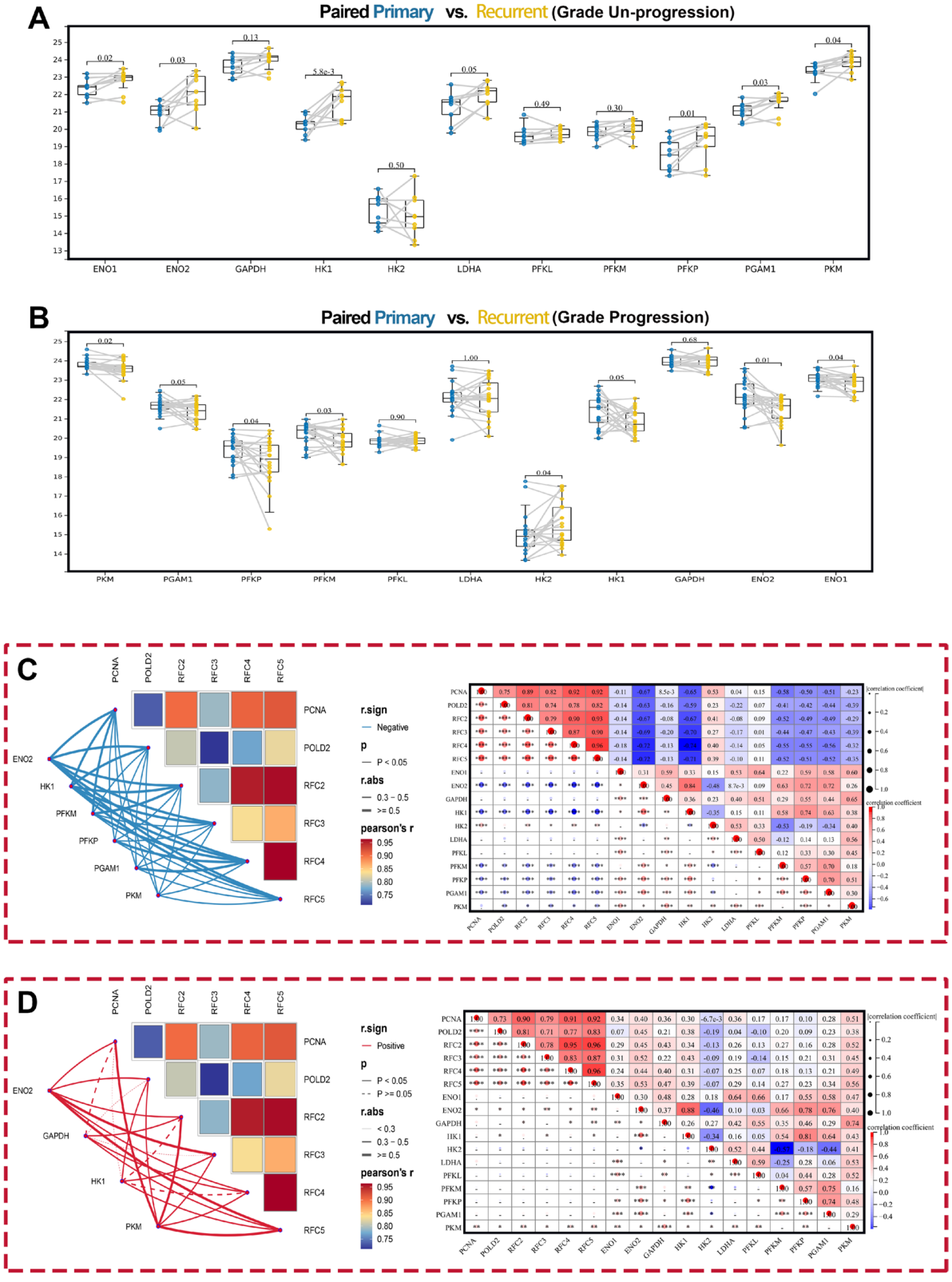

Fig. 2 The relationships between up-regulated glycolysis and non-MGMT dependent unspecific DNA damage repair system. **A** Different expression levels of key enzymes in glycolysis between paired primary-recurrent gliomas in grade un-progression group; **B** Different expression levels of key enzymes in glycolysis between paired primary-recurrent gliomas in grade progression group; **C** Correlations between the identified hub proteins of DNA damage repair system in P-A group and the key enzymes in glycolysis in P-A group; **D** Correlations between the identified hub proteins of DNA damage repair system in P-A group and the key enzymes in glycolysis in P-B group

of ATP, GTP, proteins and kinases, which were widely involved in signal transduction processes (Supplemental Table S5). Interestingly, pathway enrichment analysis demonstrated that these proteins were also widely involved in the MAPK cascade pathways and its downstream mTOR-HIF-1a-metabolic pathway (Supplemental Table S6). Then, we evaluated the expression level of key proteins in these pathways and found that the key proteins of 2 complete cascade signaling pathways were consistently abnormal expressed in T-B group, which were Ras-BRAF-MEK1/2-ERK1 and ASK1-MEKK4-p38/JNK2/3 (Fig. 3A–C). However, although the over-expressed proteins were significantly enriched in metabolic pathways, they were not solely enriched in the sugar metabolism pathway, which indicated more complex and intense "metabolic reprogramming" contributed to histological transformation (Fig. 3D).

Enhanced Non-MGMT dependent unspecific DNA damage repair pathways contributed to oligodendroglioma histological transformation

We conducted DEP analysis to discover the differences between oligodendroglioma histological transformation before and after (transformation before: T-B; transformation after: UT-A). The results demonstrated that there were 2574 (32%) DEPs between the T-A and T-B groups, among which 1950 proteins were significantly over-expressed in the T-A group (Supplemental Fig. 4A) (Supplemental Table S4). Functional analysis of these 1950 proteins demonstrated that the vast majority of

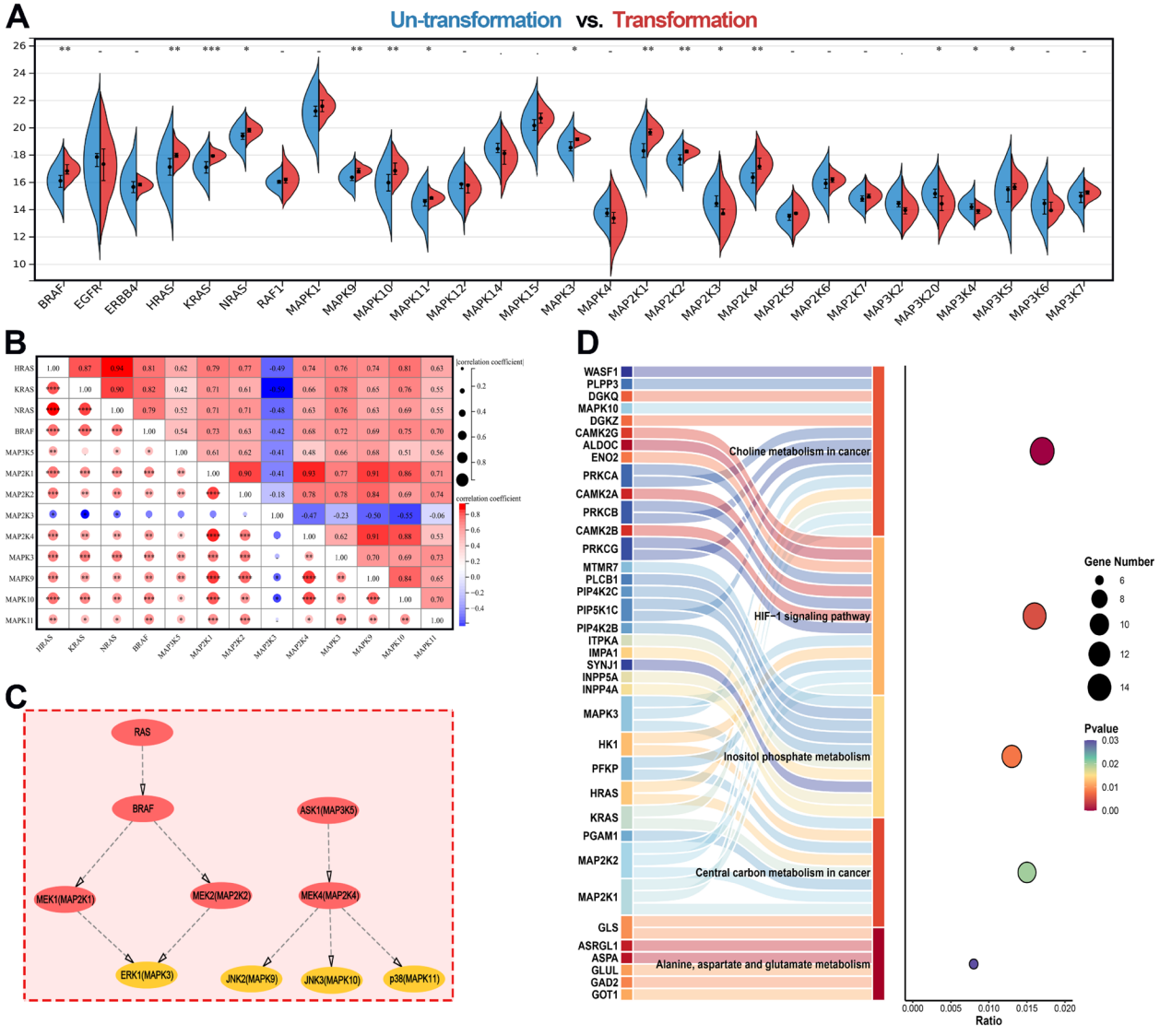

Fig. 3 The up-regulated MAPK pathways in T-B group. **A** Different expression levels of key protein kinases in MAPK pathways between T-B group and UT-B group; **B** Correlations between up-regulated key protein kinases in MAPK pathways in T-B group; **C** Tow up-regulated MAPK cascade pathways in T-B group; **D** Sankey diagram displaying proteins involved in various metabolism pathways

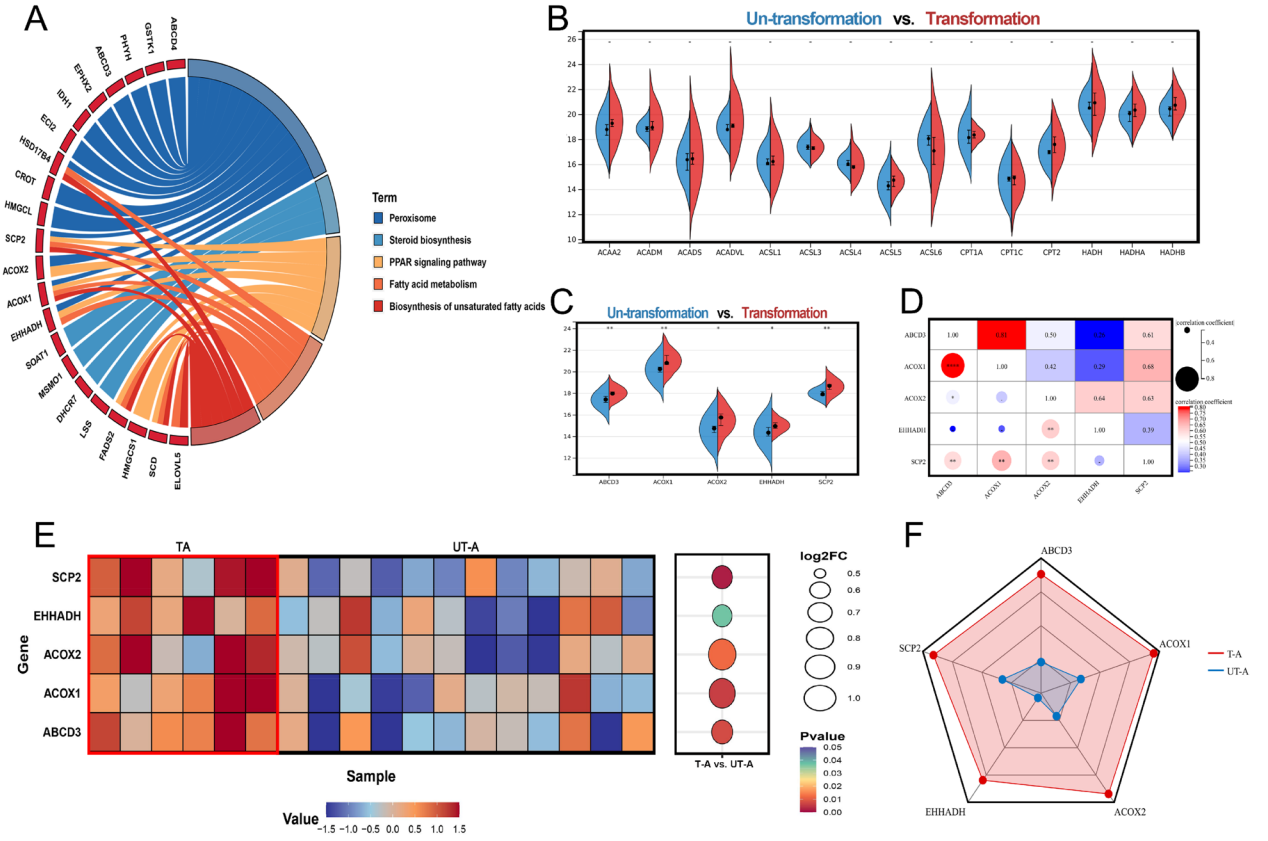

Fig. 4 The enhanced of peroxisome mediated FA beta oxidation in T-A group. **A** Enrichment circle diagram revealing proteins involved in peroxisome mediated FA metabolism pathways in KEGG; **B** Comparison of expression levels of key enzymes in mitochondria mediated FA beta oxidation between T-A and UT-A groups; **C** Comparison of expression levels of key enzymes in peroxisomes mediated FA beta oxidation between T-A and UT-A groups; **D** Correlations between key enzymes in peroxisomes mediated FA beta oxidation and ABCD3; **E** Heatmap displaying different activation levels of peroxisomes mediated FA beta oxidation between T-A and UT-A groups; **F** Radar plot of the different expression levels of key enzymes in peroxisomes mediated FA beta oxidation between T-A and UT-A groups

them were binding proteins of chromatin, DNA, RNA and protein, participating in chromatin remodeling, DNA replication, transcription, and translation processes (Supplemental Table S5). Pathway enrichment analysis revealed that these over-expressed proteins were enriched in ATP dependent chromatin remodeling, nucleotide excision repair, base excision repair, mismatch repair, DNA replication, as well as homologous and non-homologous recombination repair pathways, suggesting that strong therapy resistance characteristic of T-A group (Supplemental Fig. 4B)(Supplemental Table S6).

Further, we evaluated the MGMT level among 4 groups: histological transformation before and after, histological transformation before and after (T-B, T-A, UT-B, UT-A), and results revealed that the strong therapy resistance characteristic of T-A group was non-MGMT dependent (Supplemental Figure S4C-D). Moreover, the key proteins for DNA replication and damage repair identified above, RFC5, RFC3, RFC4, PCNA, RFC2, and POLD2, were also significantly over-expressed in the T-A group, further emphasizing the important roles of these proteins in the LGG grade progression and histological transformation (Supplemental Figure S4E).

Peroxisomal Fatty acid beta oxidation was a metabolic characteristic of gliomas after histological transformation

To investigate the differences between T-A and UT-A groups, DEP analysis was conducted. Surprisingly, only 463 (6%) proteins were found to have significant expression differences between the two groups, with 317 of them being significantly over-expressed in the T-A group (Supplemental Table S4). Functional analysis of these 317 proteins revealed that most of them were involved in fatty acid (FA) metabolism processes (Supplemental Table S5). Pathway enrichment analysis also revealed that these over-expressed proteins were enriched in lipid metabolism related pathways, including peroxisomes, steroid biosynthesis, PPAR signaling pathway, FA metabolism, and unsaturated fatty acid (UFA) biosynthesis, indicating the significant roles of "lipid metabolism reprogramming" in the histological transformation of oligodendroglioma (Fig. 4A) (Supplemental Table S6).

Due to the fact that FA beta oxidation can occur in two different organelles, mitochondria and peroxisomes, we evaluated the expression of key enzymes involved in FA beta oxidation in the two organelles between T-A and UT-A groups. Results demonstrated the key enzymes of peroxisomal FA beta oxidation, especially ACOX1, were significantly up-regulated in the T-A group, while no significant differences were found in the key enzymes of mitochondrial FA beta oxidation between the two groups (Fig. 4B, C). In addition, as ABCD3 was a lipid transport protein involved in FA oxidation and PPAR pathway localized to peroxisomes, reflecting the function and quantity of peroxisomes, we evaluated the expression level of ABCD3 between the two groups. As expect, ABCD3 was significantly up-regulated in T-A group (Fig. 4C–F). From these, we speculated that in LGG that underwent histological transformation, the ACOX1 regulated peroxisomal FA beta oxidation was significantly enhanced, which can be a metabolic characteristic of gliomas after histological transformation.

Metabolic reprogramming turned on FA metabolism during histological transformation

Based on the above analysis, we speculated that complex metabolic reprogramming may be involved in the histological transformation process of oligodendroglioma. Therefore, we divided all primary oligodendrogliomas and their paired recurrent samples into four groups, including histological transformation before (T-B), histological transformation after (T-A), histological un-transformation before (UT-B), and histological un-transformation after (UT-A) to explore the differences in metabolic processes between the four groups.

In terms of glucose metabolism, we evaluated the expression of key enzymes in aerobic glucose metabolism and glycolysis in different groups and had several findings: First, there was no significant difference in the expression of key enzymes in aerobic glucose metabolism between the T-B and UT-B groups, but the expression levels of most key enzymes in glycolysis in the T-B group were significantly higher than those in the UT-B group, including HK1, PFKP and ENO2, indicating more active glycolysis metabolism and stronger energy demand in the origination of histological transformation. Second, the expression of most key enzymes involved in glucose aerobic oxidation and glycolysis in the UT-A group demonstrated an increasing trend compared to the UT-B group, indicating that recurrent lesions had more active glucose metabolism and stronger glucose-supply energy requirement than their matched primary lesions in histological un-transformation groups. Third, in contrast to the histological un-transformation groups, the expression of most key enzymes involved in glucose aerobic oxidation and glycolysis in the T-A group displayed a downward trend compared to the T-B group, especially in the HK1, PFKP and ENO2 mediated glycolysis process, which indicated a weakening of the energy supply mode dominated by glucose metabolism after histological transformation, suggesting that histological transformation involved different metabolic and energy supply modes (Fig. 5A, B).

For lipid metabolism, we evaluated the expression of key enzymes in the mitochondrial and peroxisomal FA beta oxidation processes in different groups, and also found some differences: First, the expression of some key enzymes in mitochondrial FA beta oxidation in the T-B group was lower than that in the UT-B group, such as CPT1A and CPT2, while there was no significant difference in the expression of key enzymes in peroxisomal FA beta oxidation between the two groups; Second, no difference was observed in the expression of key enzymes in mitochondrial FA beta oxidation and peroxisomal FA beta oxidation between the UT-A group and UT-B group, indicating that the "lipid metabolism process" remained stable in the histological un-transformation group; Third, most key enzymes involved in mitochondrial FA beta oxidation and peroxisomal mediated FA beta oxidation in the T-A group displayed a significant up-regulation trend than T-B group, especially the key enzymes in peroxisomal FA beta oxidation. Meanwhile, ABCD3, which represented the function and quantity of peroxisomes, also displayed significant up-regulation. These findings suggested that oligodendroglioma histological transformation needed extra energy supply beyond glucose metabolism, and the enhanced lipid metabolism, particularly peroxisomal FA beta oxidation, played an important role in promoting oligodendroglioma histological transformation (Fig. 5C, D).

Based on the changes in key enzymes in various metabolic pathways mentioned above, we speculated that metabolic reprogramming from glycolysis to FA metabolism, especially to peroxisomal FA beta oxidation occurred during the histological transformation process. That was, metabolic reprogramming initiated FA-supply energy during the histological transformation from oligodendroglioma to astrocytoma / glioblastoma, making peroxisomal FA beta oxidation a unique metabolic characteristic of the histological transformation oligodendroglioma (Fig. 5E-F).

The enhanced synthesis of UFA promoted peroxisomal FA beta oxidation

Considering that the above displayed that the unsaturated fatty acid (UFA) synthesis pathway was enriched in T-A group, and previous studies have also proved that UFA synthesis would affect the metabolic process, especially the lipid metabolism process, therefore, we extracted the expression of key enzymes for UFA synthesis for analysis. Results revealed that when compared to

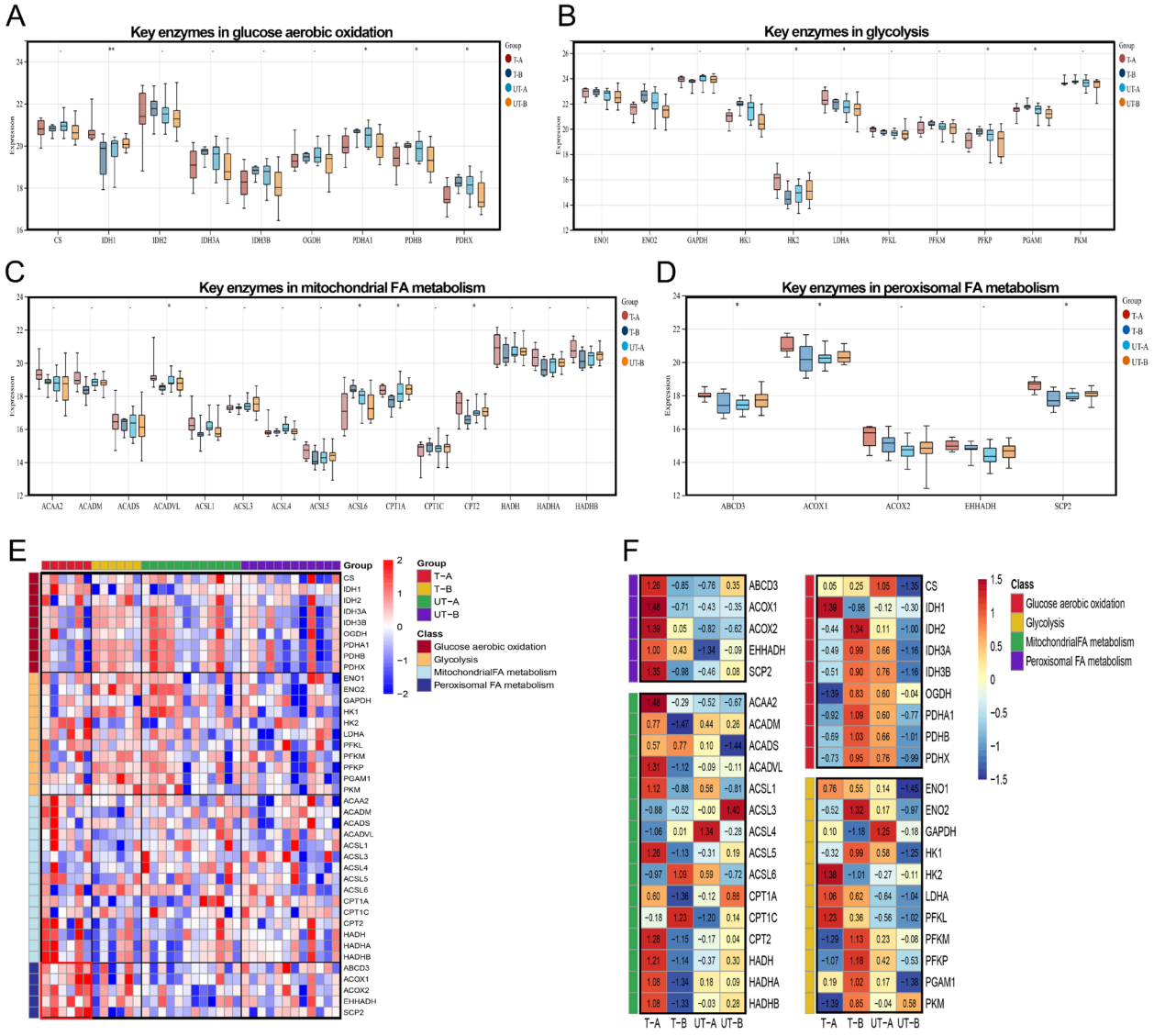

Fig. 5 Metabolic reprogramming turns on FA metabolism during histological transformation. **A** Comparison of expression levels of key enzymes in glycolysis between T-A, T-B, UT-A and UT-B groups; **B** Comparison of expression levels of key enzymes in glucose aerobic oxidation between T-A, T-B, UT-A and UT-B groups; **C** Comparison of expression levels of key enzymes in mitochondria mediated FA beta oxidation between T-A, T-B, UT-A and UT-B groups; **D** Comparison of expression levels of key enzymes in peroxisome mediated FA beta oxidation between T-A, T-B, UT-A and UT-B groups; **E** Heatmap of the expression levels of key enzymes in different metabolism pathways in T-A, T-B, UT-A and UT-B groups; **F** The average expression levels of key enzymes in different metabolism pathways in T-A, T-B, UT-A and UT-B groups

UT-A group, significant up-regulation of key enzymes involved in UFA synthesis was observed in the T-A group, suggesting a significant enhancement in the synthesis of UFA (Fig. 6A). Further analysis displayed that in the group with histological transformation (T-B and T-A), the expressions of UFA synthases such as FADS2, ELOVL5 and SCD were significantly positive correlated with that of peroxisome marker ABCD3, as well as peroxisomal FA beta oxidation rate limiting enzyme ACOX1. However, the expressions of FADS2, ELOVL5 and SCD were significantly negative correlated with that of most key enzymes involved in glycolysis (Fig. 6B, C). These results were consistent to a previous study, which uncovered that the synthesis of UFA mediated the metabolic reprogramming from glycolysis to FA metabolism of gastric cells in the process of "Metaplasia Progression to Dysplasia"[25].

In addition, compared to T-B group, the expression levels of FADS2, ELOVL5, and SCD demonstrated an obviously increasing trend in T-A group in paired difference analysis, among which, the polyunsaturated fatty acid (PUFA) elongation enzyme ELOVL5 was significantly increased (Fig. 6D). More importantly, in the comparison of all groups, the key enzymes of UFA synthesis and

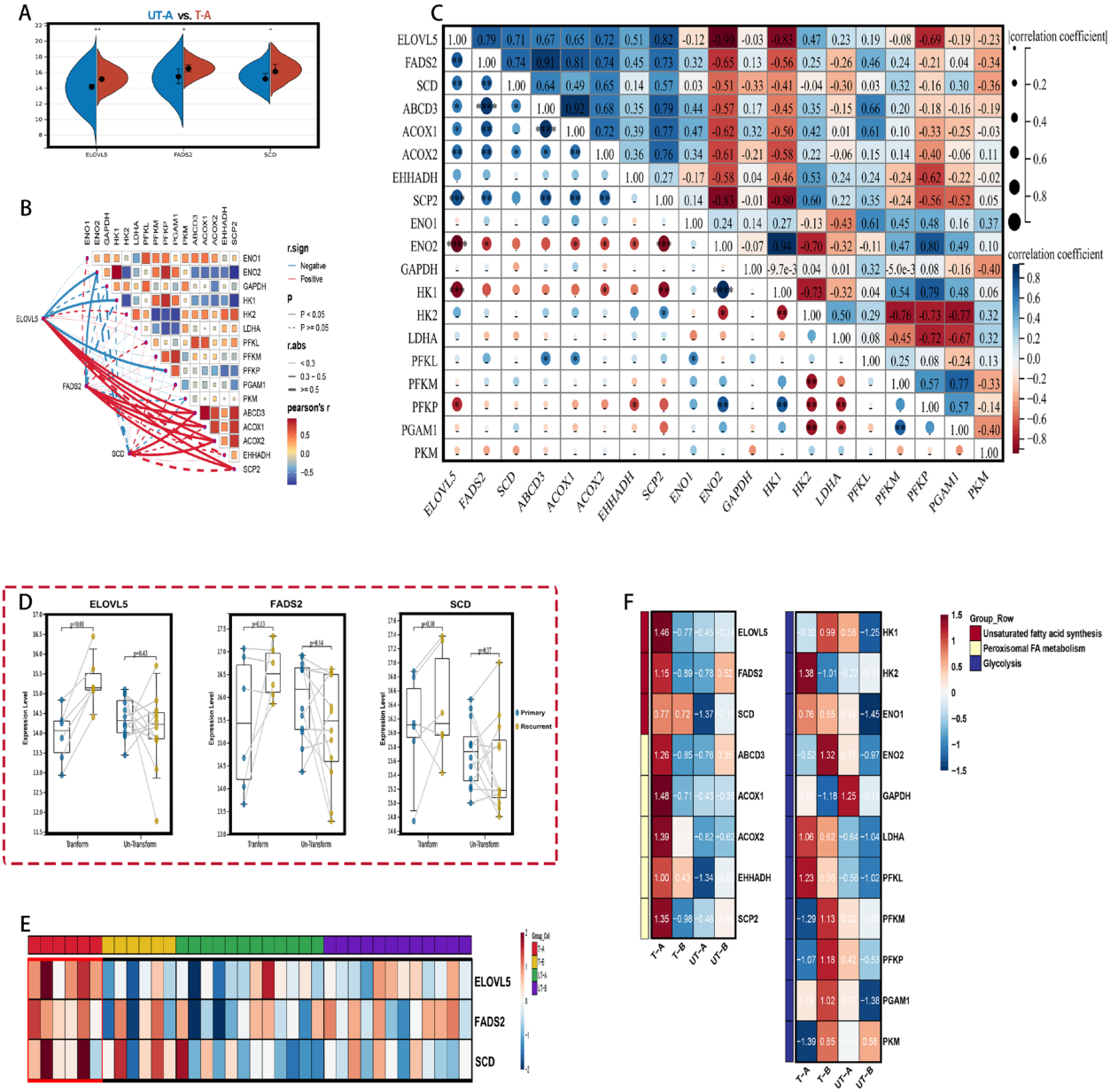

Fig. 6 The enhanced synthesis of UFA promoted peroxisome mediated FA beta oxidation. **A** Different expression levels of key enzymes in UFA synthesis between T-A and UT-A groups; **B**, **C** Correlations between the key enzymes in UFA synthesis, glycolysis and peroxisome mediated FA beta oxidation; **D** The expression levels of key enzymes in UFA synthesis between paired primary-recurrent samples in histological transformation and un-transformation groups; **E** Heatmap of expression levels of key enzymes in UFA synthesis in T-A, T-B, UT-A and UT-B groups; **F** The average expression levels of key enzymes in UFA synthesis, glycolysis and peroxisome mediated FA beta oxidation in T-A, T-B, UT-A and UT-B groups

peroxisomal FA beta oxidation displayed the highest expression levels in the T-A group (Fig. 6E, F). Therefore, we speculated that the enhanced synthesis of UFA up-regulated the function and quantity of peroxisome and may inhibit HK1-PFKP-ENO2 mediated glycolysis processes, resulting in metabolic reprogramming from glycolysis dominated to peroxisomal FA beta oxidation dominated during histological transformation. Also, due to the close relationships between UFA and membrane components, it may directly contribute to histological transformation.

The construction of LGG progression prediction model

Given that the progression of LGG was often accompanied by a dramatic deterioration of the prognosis and the following clinical therapy strategy need to be changed, we used 2 machine learning algorithms, Nearest Shrunken Centroids (NSC) and binary LASSO regression, to construct a LGG progression prediction model. 1275 DEPs

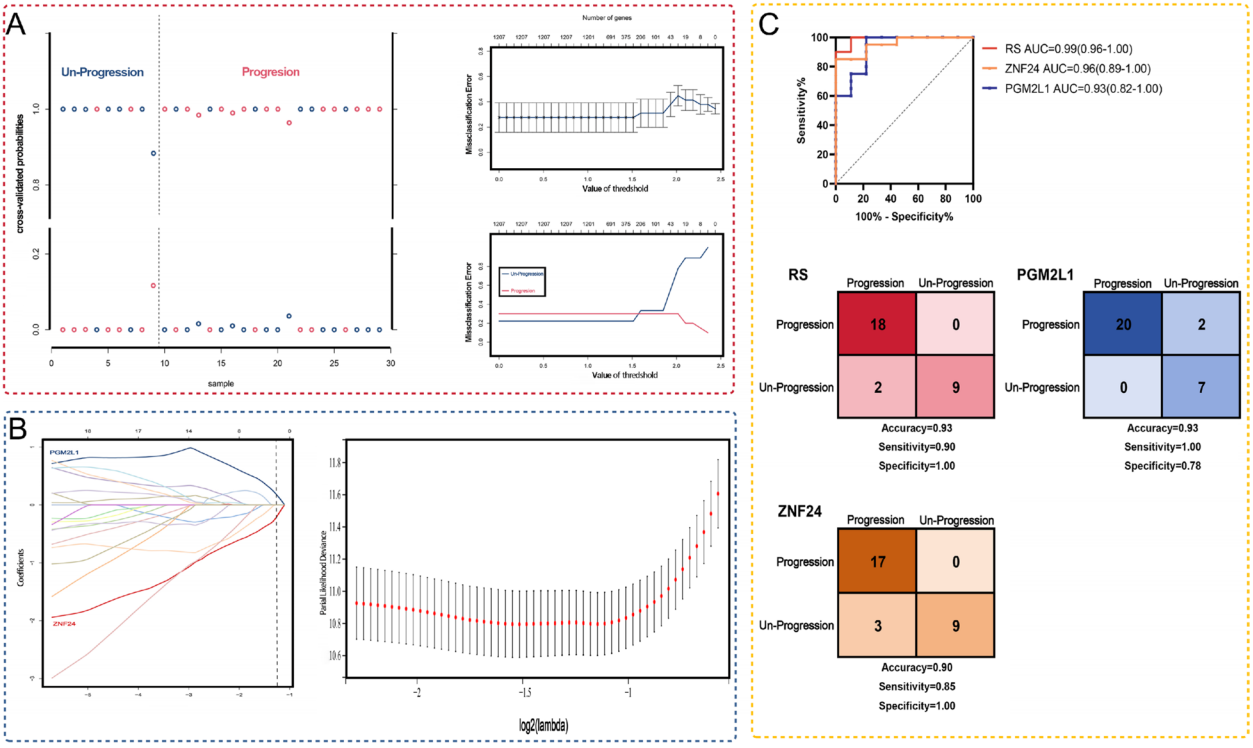

Fig. 7 The construction of LGG progression prediction model. **A** The pre-screening of proteins with potential prediction value based on NSC; **B** The Construction of LGG Progression Prediction Model based on LASSO regression; **C** ROC curves and confusion matrices validating the reliability of the LGG Progression Prediction Model

between P-B group and UP-B group were included in NSC analysis for pre-screening, and 611 proteins were identified to be with potential prediction value (Fig. 7A). Then, these proteins were included in binary LASSO regression analysis, and finally we constructed a 2-protein LGG progression prediction model, with risk score (RS) = 0.16*PGM2L1-0.18*ZNF24 (Fig. 7B). The two-protein classifier reached an AUC of 99% based on the receiver operating characteristic (ROC) curve analysis with 93% accuracy, 90% sensitivity and 100% specificity. More importantly, both the PGM2L1 and ZNF24 displayed independent predictive value, which greatly increased their clinical values. PGM2L1 reached an AUC of 93% based on the ROC with 93% accuracy, 100% sensitivity and 78% specificity, while ZNF24 reached an AUC of 96% based on the ROC with 90% accuracy, 85% sensitivity and 100% specificity (Fig. 7D).

Discussion

Gliomas of different histological types and WHO grades have varying impacts on the prognosis of patients [26]. Obviously, grade progression and histological transformation can affect the prognosis of patients, therefore, studying the molecular mechanisms underlying the progression of LGG was of great significance for exploring the optimal treatment plan and improving patient prognosis in the future. However, due to the difficulty in obtaining paired primary-recurrent grade progression / histological transformation LGG samples, lacking enough studies explored this crucial issue. Based on the above, this study had several advantages as follow. Firstly, as far as we know, this was the first study that focused on proteomics characteristics to elucidate the mechanisms of LGG grade progression and histological transformation. Secondly, our study obtained a considerable number of paired samples. Thirdly, our study evaluated the metabolic characteristics of various types of LGG at protein expression levels by compared key enzymes in various major metabolic pathways, and uncovered the important roles of metabolic reprogramming in the LGG grade progression/histological transformation, providing a direction for subsequent research.

In this study, we emphasized that the up-regulations of MAPK signaling pathways in primary LGG contributed to both grade progression and histological transformation. Specifically, the up-regulation of two complete MAPK cascade pathways in primary LGG, Ras-BRAF-MEK1/2-ERK1/2 and ASK1-MEK4-p38/JNK2/3, promoted grade progression, and the degree of up-regulations of these two MAPK cascade pathways significantly affected the grade progression span. Similarly, we emphasized the up-regulation of two complete MAPK cascade pathways in primary oligodendroglioma, Ras-BRAF-MEK1/2-ERK1 and ASK1-MEK4-p38/JNK2/3,

promoted histological transformation. Previous studies have proved that MAPK cascade pathways regulated cellular events directly related to tumor development, such as proliferation, apoptosis, inflammation, and immunity [27, 28]. JNKs and ERKs have been described as the main participants in the carcinogenic process [29, 30]. In gliomas, the abnormal activation of MAPK pathways has been proven to support the infiltration, proliferation, and migration of GBM cells [31]. More importantly, the abnormal activation of the MAPK pathway has been recognized as an initiation event for most LGG in children [32, 33]. At present, many studies have proposed the usage of MAPK inhibitors combined with TMZ for glioma therapy [34, 35]. Our study, for the first time, emphasized the important roles of abnormal up-regulation of the Ras/p38-MAPK pathways in promoting LGG grade progression and histological transformation, and discovered two complete abnormally up-regulated cascade pathways, providing a theoretical basis for targeted inhibition therapy of MAPKs in gliomas in the future.

Till now, the standard therapy strategies for glioma after surgery was oral TMZ combined with radiation therapy, and their effects were non-selective DNA damage, which led to therapy resistance after recurrence [36]. Our results correspond to the above statement. Especially, high expression levels of DNA damage repair related proteins were significantly enriched in the T-A and P-A groups, indicating that therapy resistance was an important cause of LGG grade progression and histological transformation during recurrence. It was widely recognized that the methylation of MGMT was a key molecular event in evaluating the sensitivity of patients to TMZ treatment [17, 18]. Patients with MGMT promoter methylation were considered low MGMT expressed and sensitive to TMZ [37]. However, in clinical practice, many patients with MGMT methylation still suffered from recurrence, grade progression and histological transformation after standard treatment. Our results uncovered that activation of non-MGMT dependent unspecific DNA damage repair systems, such as base excision repair, mismatch repair and nucleotide excision repair, were important supporters of therapy resistance. They can not only counteract DNA damage caused by TMZ, but also repaired DNA damage caused by radiation, exerting a dual resistance to treatment. More importantly, our study identified that RFC5, RFC3, RFC4, PCNA, RFC2, and POLD2 were involved in all the above DNA damage repair processes and DNA replication process. Previous studies revealed that RFC5, RFC3, RFC4, and RFC2 formed RFC complex that can bind to PCNA to form a sliding clip structure, helping DNA polymerase move and replicate on the DNA strand [19–22]. Also, RFC complex itself can bind to cell cycle checkpoint proteins to initiate signal transduction downstream of DNA damage checkpoints, thereby counteracting the damage of DNA [24, 38]. Our findings emphasized that the up-regulation of unspecific DNA damage repair pathways mediated by the RFC complex was a major cause in the development of treatment resistance (including TMZ and radiotherapy resistance) in LGG, leading to grade progression and histological transformation. This mechanism of treatment resistance did not depend on the expression of MGMT, but rather on the biological characteristics of the tumor itself.

It was worth noting that this study evaluated the expression levels of key enzymes in various metabolic pathways to reflect their activities, and found that complex metabolic reprogramming affected the grade progression and histological transformation. It was already known that metabolic reprogramming was one of the markers of cancer, playing a crucial role in reshaping tumor immune microenvironment, enhancing tumor treatment resistance, and promoting tumor progression [39–41]. Compared to non-tumor tissues, tumor tissues exhibited metabolic changes as each behavior of cancer cells, such as proliferation, invasion, and metastasis, required reprogramming of their metabolic state [42, 43]. At present, the most extensively studied example of metabolic reprogramming in cancer cells was aerobic glycolysis, also known as the "Warburg effect": an increase in the rate of glycolysis and lactate production in cancer cells even in the presence of oxygen [44]. Our study revealed that high levels of key enzymes in glycolysis in primary LGG promoted grade progression and histological transformation during recurrence, especially, the up-regulation of HK1-PFKP-ENO2 mediated glycolysis processes. Interestingly, previous studies have emphasized the enhancement of glycolysis levels mediated by HK2 in various cancers [15, 16], while our study did not find meaningful over-expression of HK2 during the LGG grade progression and histological transformation processes. Moreover, our results revealed the positive relationships between the level of glycolysis in primary LGG and the activation of unspecific DNA damage repair systems in their match recurrent LGG. The possible explanation for this result can be that during the primary stage, the stronger the glycolysis process, the more acidic microenvironment provided by the tumor. On the one hand, acidic microenvironment enhanced the malignancy of the tumor itself (extracellular matrix remodeling, angiogenesis, and tumor invasion) and laid the foundation for grade progression and histological transformation; On the other hand, it enhanced the therapeutic resistance potential of tumors and provided sufficient energy to activate unspecific DNA damage repair system and supported DNA replication process regulated by RFC complex.

More importantly, our results uncovered for the first time that the energy metabolism of oligodendroglioma undergone a shift from glycolysis dominated to peroxisomal FA beta oxidation dominated during histological transformation, and the enhanced synthesis of UFA may be the initiation factor. Currently, studies have revealed that the accumulation of monounsaturated fatty acids (MUFA) can up-regulate the quantity and ability of peroxisome, alter cell membrane composition, and regulate cell differentiation [45, 46]. Our results suggested that synthesis enzymes of MUFA, such FASD2 and SCD were significantly up-regulated in the T-A group and displayed strong positive correlations with ABCD3 and ACOX1. Similar to our results, Yoonkyung Won et al. [25]. have found that metabolic reprogramming from glycolysis to FA metabolism occured during the progression of gastric metaplasia to dysplasia, and this process relied on the synthesis of MUFA mediated by SCD. However, different to their result, our analysis revealed that the expression of polyunsaturated fatty acids (PUFA) synthase, ELOVL5, was most significantly up-regulated in the T-A group, whose expression negatively correlated with HK1-PFKP-ENO2 mediated glycolysis level but positively correlated with peroxisomal FA beta oxidation level. This result suggested that the metabolic reprogramming during oligodendroglioma histological transformation may be more dependent on the synthesis of PUFA mediated by ELOVL5.

Innovatively, our analysis established a robust two-protein LGG progression prediction model, which was proved to have a remarkable prediction ability. The combination or alone of the two proteins all displayed extremely high predictive efficacy, with accuracies of more than 90%, making them potential biomarkers of LGG progression for clinical monitoring and treatment. In terms of specific proteins included in the model, PGM2L1 was identified as a promoter of LGG progression, while ZNF24 was identified as a protective factor. PGM2L1 was a glucose-1,6-diphosphate synthase [47], which was mainly involved in the regulation of brain energy metabolism [48]. Latest study had revealed that under hypoxic condition, tumor-associated fibroblasts up-regulated PGM2L1 in triple-negative breast cancer (TNBC) cells via secreting CSF3, enhancing PGM2L1-dependent glycolysis reprogramming, and ultimately promoted the progression and metastasis of TNBC [49]. ZNF24 was a member of the Kruppel-like zinc finger transcription factor family [50], and its tumor inhibition ability has been noted in breast cancer, pancreatic cancer and lung cancer. As a transcription factor, ZNF24 can inhibit the transcription of VEGF-A and play a tumor suppressor role by inhibiting angiogenesis [51–53]. Moreover, abnormal expression of ZNF24 can negatively regulate the expression of p65 and block lung cancer cells in S phase, inhibiting tumor growth [54]. These existing results further verified the reliability of our two-protein model. However, the relevant research on these two proteins was still not enough, and lacking studies explored their specific functions and mechanisms in glioma. Therefore, the follow-up research on these two proteins in glioma progression was still in urgent need. But the valuable thing was that, till now, effective model of LGG progression prediction remained urgent and unmet needs, our LGG progression prediction model, based on 2 protein biomarkers, was a relatively easy and practicable technique for subsequent application.

Limitations

Although the 2-protein prediction model were constructed based on a tenfold cross validation and exhibited high prediction value, due to lacking enough relevant studies, external validation did not conducted. In future, large-scale prospective studies to validate our 2-protein prediction model in a larger sample size were in urgent need.

Conclusion

In summary, this study provided an overview of LGG grade progression and histological transformation at proteomics level, uncovering that glioma grade progression and histological transformation were complex biological processes, which involved the abnormal up-regulation of Ras/p38-MAPK signalings, enhanced non-MGMT dependent unspecific DNA damage repair system regulated by RFC complex and metabolic reprogramming based on HK1-PFKP-ENO2 mediated glycolysis and peroxisomal FA beta oxidation. Meanwhile, we identified PGM2L1 and ZNF24 as potential biomarkers for LGG progression, providing novel biomarkers of LGG progression for clinical monitoring and developing new therapy strategies.

Methods

Sample acquirement

We retrospectively collected formalin-fixed and paraffin-embedded (FFPE) human brain glioma samples from the Department of Pathology, Zhujiang Hospital. The acquisition of samples was approved by the Ethics Committee of Zhujiang Hospital of Southern Medical University (2025-SJWK-004). The study was conducted according to the principles of the Declaration of Helsinki. All participants provided written informed consent.

Inclusion criteria and survival data collection

All the included samples must meet the following criteria: 1. Glioma samples that must be diagnosed by pathology; 2. All primary samples must be matched by recurrent samples; 3. none of the patients had received

any prior treatment before first surgery, such as radiotherapy or chemotherapy; 4. All the patients received post-operative oral TMZ and radiotherapy (to avoid DEPs caused by therapy). The survival information of all patients was followed up by telephone, including overall survival (OS), recurrent free survival (RFS) and post recurrent survival (PRS).

Public datasets

The glioma patients' clinical information were downloaded from The Cancer Genome Atlas database (TCGA, https://protal.gdc.cancer.gov/). The clinical information of glioma patients from CGGA mRNAseq_693 dataset and glioma patients from the CGGA mRNAseq_325 dataset were downloaded from Chinese Glioma Genome Atlas (CGGA, http://www.cgga.org.cn/).

Sample handling

Paraffin-embedded tissues, paraffin sections

Take 10 paraffin sections and follow the instructions for the dewaxing agent (Biosharp Biotechnology Co., Ltd.). After dewaxing, grind the samples into powder, add 100 µl SDT lysis buffer, heat at 95 °C for 90 min, cool at room temperature, perform ultrasonic lysis in an ice-water bath for 5 min, and centrifuge at 15000 g to collect the supernatant protein solution. Finally, determine the protein concentration using a BCA assay kit.

Proteolytic desalting

Start by taking 100 ug of protein solution based on protein concentration, then adjust the volume to 200 µl with 8 M urea, followed by reduction with 5 mM DTT at 37 °C for 45 min, and alkylation with 11 mM iodoacetamide (IAM) in a dark room at room temperature for 15 min. Then, add 800 µl of 25 Mm ammonium bicarbonate solution and 2 µl of Trypsin (Promega, V5280), and digest overnight at 37 °C. Adjust the pH of the digested peptides to 2–3 using 20%TFA, followed by desalting with C18 (Millipore, Billerica, MA) resin. Finally, determine the peptide concentration using a Pierce™ Quantitative Peptide Assay Kit with standards (Thermo Fisher).

LC–MS/MS analysis

Liquid chromatography detection

Samples were separated using the Vanquish Neo UHPLC liquid chromatography system. The mobile phase A consisted of 0.1% formic acid aqueous solution, while mobile phase B was 100% acetonitrile containing 0.1% formic acid. The injection mode employed a trap-and-elute dual-column method, with a PepMap Neo Trap Cartridge (300 µm * 5 mm, 5 µm) as the trapping column and an Easy-Spray™ PepMap™ Neo UHPLC column (150 µm * 15 cm, 2 µm) as the analytical column. The column temperature was controlled at 55 °C, with an injection volume of 200 ng, a flow rate of 2.5 µl /min, an effective gradient of 22 min, and a total runtime of 24 min. Orbitrap Astral Mass Spectrometry Detection DIA analysis utilized the Vanquish Neo system (Thermo Fisher Scientific) for chromatographic separation. Samples separated by nano-flow high-performance liquid chromatography were subjected to DIA (Data-Independent Acquisition) mass spectrometry analysis using the Orbitrap Astral high-resolution mass spectrometer (Thermo Scientific). The detection mode was positive ion mode, with a precursor ion scan range of 380–980 m/z, a primary mass resolution of 240,000 at 200 m/z, a Normalized AGC Target of 500%, and a Maximum IT of 5 ms. MS2 was performed using DIA data acquisition mode, with 299 scan windows, an Isolation Window of 2 Th, HCD Collision Energy of 25%, a Normalized AGC Target of 500%, and a Maximum IT of 3 ms.

Database search and quantification

MS raw data were analyzed using DIA-NN (v1.8.1) with library-free method. The uniprotkb_proteome_UP000005640_human_82493_20240528.fasta database (A total of 82,493 sequences) was used to create a spectra library with deep learning algorithms of neural networks. the option of MBR (Match Between Runs) was employed to create a spectral library from DIA data and then reanalyzed using this library. FDR (false discovery rate) of search results was adjusted to < 1% at both protein and precursor ion levels, the remaining identifications were used for further quantification analysis. Label-free protein quantifications (LFQ) were calculated using MaxLFQ algorithm. Quantification will be performed using razor and unique peptides, including those modified by acetylation (protein N-terminal), oxidation (Met) and deamidation (NQ). LFQ intensity values in the output tables reflect the relative abundance of each protein across different samples or conditions.

Preprocessing of proteomics datasets

Protein intensities were log2 transformed for downstream statistical and bioinformatics analysis [55]. Proteomics datasets were then filtered for 75% valid values across all samples (proteins with > 25% missing values were excluded from downstream statistical analysis). To impute missing values, the "DreamAI package" was used to perform an imputation of the proteins. The resulting global proteomics numbering 8067 was used for downstream analysis.

Differential proteomics analysis

Differential expressed protein (DEP) analysis was conducted by using "limma package" (version 3.40.6). Proteins with |fold change (FC)| larger than 1.5 between two groups and p values less than 0.05 were considered DEPs.

Functional annotation and enrichment analysis

Functional analysis was based on Gene Ontology and pathway enrichment analysis was based on Kyoto Encyclopedia of Genes and Genomes. Both functional analysis and pathway enrichment analysis were conducted via the Database for Annotation, Visualization, and Integrated Discovery (https://davidbioinformatics.nih.gov) [56]. Gene Set Enrichment Analysis (GSEA) were conducted to evaluate the difference of pathway enrichment between the two groups [57]. Single-sample geneset enrichment analysis (ssGSEA) were conducted to evaluate the enrichment score of each sample in each gene set. Molecular Signatures Database (MSigDB) of KEGG gene sets (C2) was used for enrichment analysis. Pathways with |NES| larger than 1, p value less than 0.05 and an FDR less than 0.25 were considered statistically significant.

Construction of machine learning-based classifiers

First, the initial number of features was reduced by the nearest shrunken centroid (NSC) algorithms via R package "pamr". A tenfold cross-validation and 1000 iterations strategy was conducted to select features. The features were included in LASSO regression for binary classification via R package "glmnet". A tenfold cross-validation strategy was also conducted in this process. The threshold of feature selection is based on the minimum amount of protein included with the highest Area Under the Curve (AUC) of Receiver Operating Curve (ROC). The calculation and visualization AUC of ROC were achieved by Prism 9.0, which also help to calculated the best threshold of each feature. Based on the best threshold of each feature, confusion matrices were constructed to examine the classification accuracy of each feature.

Survival analysis

Kaplan–Meier survival curves (log-rank test) were used for survival analysis by R package "survival".

Statistical analysis

R version 4.4.1 (https://www.r-project.org/) and free online platforms, Metware Cloud (https://cloud.metware.cn) and Sangerbox (http://www.sangerbox.com) [58], were used for our statistical analysis and results visualization. Pearson's correlation was used for continuous variables. Wilcoxon rank-sum test was used for continuous variables and rank variables, while paired t-test was used for the comparison of pairwise primary-recurrent samples. All tests were two-tailed, and p values less than 0.05 or FDR less than 0.25 were considered statistically significant.

Abbreviations

LGG	Low-grade glioma
TMZ	Temozolomide
METex14	MET-exon-14-skipping
DEP	Differential expressed protein
P-B	Grade progression before
P-A	Grade progression after
UP-B	Grade un-progression before
UP-A	Grade un-progression after
FA	Fatty acid
UFA	Unsaturated fatty acid
PUFA	Polyunsaturated fatty acid
MUFA	Monounsaturated fatty acids
T-B	Histological transformation before23
T-A	Histological transformation after
UT-B	Histological un-transformation before
UT-A	Histological un-transformation after
NSC	Nearest Shrunken Centroids
ROC	Receiver operating characteristic
TNBC	Triple-negative breast cancer
FFPE	Formalin-fixed and paraffin-embedded

Supplementary Information

The online version contains supplementary material available at https://doi.org/10.1186/s40246-026-00945-8.

Supplementary Material 1: Supplemental Figure S1 Over view. (A) The length distribution of the peptide segments identified by mass spectrometry; (B) Protein qualitative and quantitative results based on mass spectrometry data through DIA-NN (v1.8.1) software; (C) The distribution of abundance values after normalization of all samples; (D) Prognostic stratification based on glioma histological type through K-M analysis; (E) Prognostic stratification based on glioma WHO grade through K-M analysis; (F) Proteomics expression patterns of different types of glioma.

Supplementary Material 2: Supplemental Figure S2 The enrichment of MAPK-related pathways in P-B group. (A) Result of GSEA analysis between P-B and UP-B groups; (B) Heatmap of ssGSEA analysis displaying enrichment levels of different pathways in each sample; (C) Sankey diagram displaying up-regulated proteins in P-B groups involved in MAPK-related pathways; (D) Enrichment circle diagram revealing proteins involved in HIF-1a downstream metabolism pathways.

Supplementary Material 3: Supplemental Figure S3 The enhancing Non-MGMT dependent unspecific DNA damage repair contributed to LGG grade progression. (A) Volcanic plot of DEP analysis between P-A and P-B group; (B) Volcanic plot of DEP analysis between P-A and UP-A group; (C) Bubble chart displaying the enrichment of unspecific DNA damage repair pathways in P-A group; (D) Comparison of MGMT expression levels between paired primary-recurrent LGG samples in grade progression and un-progression groups; (E) Comparison of MGMT expression levels between progression and un-progression groups; (F) Enrichment circle diagram revealing up-regulated proteins(P-A vs. UP-A) involved in unspecific DNA damage repair pathways; (G) Enrichment circle diagram revealing up-regulated proteins(P-A vs. P-B) involved in unspecific DNA damage repair pathways; (H) PPI network of hub up-regulated proteins participating in non-MGMT dependent unspecific DNA damage repair pathways in P-A group; (I) Sankey diagram displaying hub proteins involved in pathways enriched in P-A group; (J) Radar plot displaying the different expression levels of hub proteins in unspecific DNA damage repair pathways between P-A and P-B group; (K) Radar plot displayinng the different expression levels of hub proteins in unspecific DNA damage repair pathways between P-A and UP-A group.

Supplementary Material 4: Supplemental Figure S4 The enhancing Non-MGMT dependent unspecific DNA damage repair contributed to LGG histological transformation. (A) DEP analysis between T-A and T-B groups; (B) Bubble chart displaying the enrichment of unspecific DNA damage repair pathways in each comparison group; (C) The expression level of MGMT between paired primary-recurrent samples in histological transformation and un-transformation groups; (D) Comparison of MGMT expression levels between histological transformation and un-transformation groups; (E) Sankey diagram displaying up-regulated proteins (T-A vs. T-B) involved in unspecific DNA damage repair pathways.

Supplementary Material 5: Supplemental Table S1 Details of samples in

Zhujiang cohort.

Supplementary Material 6: Supplemental Table S2 Clinical information of patients in Zhujiang cohort.

Supplementary Material 7: Supplemental Table S3 Grouping of samples.

Supplementary Material 8: Supplemental Table S4 Results of DEPs (|FC|>1.5, p<0.05) in each analysis.

Supplementary Material 9: Supplemental Table S5 GO enrichment results of up-regulated DEPs in each analysis.

Supplementary Material 10: Supplemental Table S6 KEGG enrichment results of up-regulated DEPs in each analysis.

Supplementary Material 11: Supplemental Table S7 Log2 transformed proteomics expression matrix of Zhujiang Cohort.

Acknowledgements
We are grateful for the support from the Department of Pathology, Zhujiang Hospital, Southern Medical University.

Author contributions
QH, TC and YK were responsible for the study design, revision or critical review of the article and gave final approval of the version to be published; JL, XS, SS and HL took part in the drafting, data analysis and interpretation. All authors have agreed on the journal to which the article has been submitted and agree to be accountable for all aspects of the work.

Funding
Taoliang Chen received funding from the Natural Science Foundation of China (No. 82103668) and Guangzhou Science and Technology Planning Project (No. 2024A04J9993). Jie Liu received funding from Guangzhou Science and Technology Planning Project (No. 2024A04J4878) and President Foundation of Zhujiang Hospital, Southern Medical University (No. yzjj2022qn11).

Data availability
All data needed to evaluate the conclusions in the paper are present in the paper and/or the Supplementary Materials. The standardlized proteomics matrix was provided in Supplemental Table 7. There are no custom computer codes or scripts used to generate results reported in the manuscript. Any additional information required to reanalyze the data reported in this paper is available from the lead contact upon request.

Declarations

Ethics approval and consent to participate
The acquisition of samples was approved by the Ethics Committee of Zhujiang Hospital of Southern Medical University (2025-SJWK-004). The study was conducted according to the principles of the Declaration of Helsinki. All participants provided written informed consent.

Consent for publication
All authors have read and approved the manuscript.

Competing interests
The authors declare no competing interests.

Author details
[1]The National Key Clinical Specialty, The Engineering Technology Research Center of Education Ministry of China, Guangdong Provincial Key Laboratory On Brain Function Repair and Regeneration, Department of Neuro-oncological Surgery, Zhujiang Hospital, Southern Medical University, Guangzhou 510282, China
[2]Neuromedical Center, School of Medicine, the Sixth Affiliated Hospital of South China University of Technology (Nanhai District People's Hospital of Foshan), 528200 Foshan, China

Received: 1 January 2026 / Accepted: 26 February 2026
Published online: 10 March 2026

References

1. Schaff LR, Mellinghoff IK. Glioblastoma and other primary brain malignancies in adults: a review. JAMA. 2023;329(7):574–87. https://doi.org/10.1001/jama.2023.0023.
2. Louis DN, Perry A, Wesseling P, Brat DJ, Cree IA, Figarella-Branger D, et al. The 2021 WHO classification of tumors of the central nervous system: a summary. Neuro Oncol. 2021;23(8):1231–51. https://doi.org/10.1093/neuonc/noab106.
3. van den Bent MJ, Geurts M, French PJ, Smits M, Capper D, Bromberg JEC, et al. Primary brain tumours in adults. Lancet. 2023;402(10412):1564–79. https://doi.org/10.1016/s0140-6736(23)01054-1.
4. Wang J, Cazzato E, Ladewig E, Frattini V, Rosenbloom DI, Zairis S, et al. Clonal evolution of glioblastoma under therapy. Nat Genet. 2016;48(7):768–76. https://doi.org/10.1038/ng.3590.
5. Brat DJ, Verhaak RG, Aldape KD, Yung WK, Salama SR, Cooper LA, et al. Comprehensive, integrative genomic analysis of diffuse lower-grade gliomas. N Engl J Med. 2015;372(26):2481–98. https://doi.org/10.1056/NEJMoa1402121.
6. Bai H, Harmancı AS, Erson-Omay EZ, Li J, Coşkun S, Simon M, et al. Integrated genomic characterization of IDH1-mutant glioma malignant progression. Nat Genet. 2016;48(1):59–66. https://doi.org/10.1038/ng.3457.
7. Zhang RR, Pointer KB, Kuo JS, Dempsey RJ. Mutational analysis reveals the origin and therapy-driven evolution of recurrent glioma. Neurosurgery. 2014;75(6):9–10. https://doi.org/10.1227/neu.0000000000000580.
8. Mazor T, Pankov A, Johnson BE, Hong C, Hamilton EG, Bell RJA, et al. DNA methylation and somatic mutations converge on the cell cycle and define similar evolutionary histories in brain tumors. Cancer Cell. 2015;28(3):307–17. https://doi.org/10.1016/j.ccell.2015.07.012.
9. Mazor T, Chesnelong C, Pankov A, Jalbert LE, Hong C, Hayes J, et al. Clonal expansion and epigenetic reprogramming following deletion or amplification of mutant IDH1. Proc Natl Acad Sci U S A. 2017;114(40):10743–8. https://doi.org/10.1073/pnas.1708914114.
10. Hu H, Mu Q, Bao Z, Chen Y, Liu Y, Chen J, et al. Mutational landscape of secondary glioblastoma guides MET-targeted trial in brain tumor. Cell. 2018;175(6):1665-78.e18. https://doi.org/10.1016/j.cell.2018.09.038.
11. Zhang H, Liu T, Zhang Z, Payne SH, Zhang B, McDermott JE, et al. Integrated proteogenomic characterization of human High-Grade Serous Ovarian Cancer. Cell. 2016;166(3):755–65. https://doi.org/10.1016/j.cell.2016.05.069.
12. Zhang B, Wang J, Wang X, Zhu J, Liu Q, Shi Z, et al. Proteogenomic characterization of human colon and rectal cancer. Nature. 2014;513(7518):382–7. https://doi.org/10.1038/nature13438.
13. Mertins P, Mani DR, Ruggles KV, Gillette MA, Clauser KR, Wang P, et al. Proteogenomics connects somatic mutations to signalling in breast cancer. Nature. 2016;534(7605):55–62. https://doi.org/10.1038/nature18003.
14. Berger TR, Wen PY, Lang-Orsini M, Chukwueke UN. World Health Organization 2021 classification of Central Nervous System tumors and implications for therapy for Adult-Type Gliomas: a review. JAMA Oncol. 2022;8(10):1493–501. https://doi.org/10.1001/jamaoncol.2022.2844.
15. Xu S, Catapang A, Doh HM, Bayley NA, Lee JT, Braas D, et al. Hexokinase 2 is targetable for HK1 negative, HK2 positive tumors from a wide variety of tissues of origin. J Nucl Med. 2018;60(2):212–7. https://doi.org/10.2967/jnumed.118.212365.
16. Ciscato F, Ferrone L, Masgras I, Laquatra C, Rasola A. Hexokinase 2 in cancer: a prima donna playing multiple characters. Int J Mol Sci. 2021. https://doi.org/10.3390/ijms22094716.
17. Tomar MS, Kumar A, Srivastava C, Shrivastava A. Elucidating the mechanisms of Temozolomide resistance in gliomas and the strategies to overcome the resistance. Biochim Biophys Acta Rev Cancer. 2021;1876(2):188616. https://doi.org/10.1016/j.bbcan.2021.188616.
18. Wu S, Li X, Gao F, de Groot JF, Koul D, Yung WKA. PARP-mediated PARylation of MGMT is critical to promote repair of temozolomide-induced O6-methylguanine DNA damage in glioblastoma. Neuro Oncol. 2021;23(6):920–31. https://doi.org/10.1093/neuonc/noab003.
19. Li Y, Gan S, Ren L, Yuan L, Liu J, Wang W, et al. Multifaceted regulation and functions of replication factor C family in human cancers. Am J Cancer Res. 2018;8(8):1343–55.
20. Schrecker M, Castaneda JC, Devbhandari S, Kumar C, Remus D, Hite RK. Multistep loading of a DNA sliding clamp onto DNA by replication factor C. Elife. 2022. https://doi.org/10.7554/eLife.78253.
21. Kang S, Yoo J, Myung K. PCNA cycling dynamics during DNA replication and repair in mammals. Trends Genet. 2024;40(6):526–39. https://doi.org/10.1016/j.tig.2024.02.006.

22. Liu L, Tao T, Liu S, Yang X, Chen X, Liang J, et al. An RFC4/Notch1 signaling feedback loop promotes NSCLC metastasis and stemness. Nat Commun. 2021;12(1):2693. https://doi.org/10.1038/s41467-021-22971-x.
23. Bowman GD, O'Donnell M, Kuriyan J. Structural analysis of a eukaryotic sliding DNA clamp-clamp loader complex. Nature. 2004;429(6993):724–30. https://doi.org/10.1038/nature02585.
24. Alaa Eldeen M, Mamdouh F, Abdulsahib WK, Eid RA, Alhanshani AA, Shati AA, et al. Oncogenic potential of Replication Factor C Subunit 4: correlations with tumor progression and assessment of potential inhibitors. Pharmaceuticals (Basel). 2024. https://doi.org/10.3390/ph17020152.
25. Won Y, Jang B, Lee SH, Reyzer ML, Presentation KS, Kim H, et al. Oncogenic fatty acid metabolism rewires energy supply chain in gastric carcinogenesis. Gastroenterology. 2024;166(5):772-86.e14. https://doi.org/10.1053/j.gastro.2024.01.027.
26. Ostrom QT, Cioffi G, Gittleman H, Patil N, Waite K, Kruchko C, et al. CBTRUS statistical report: primary brain and other central nervous system tumors diagnosed in the United States in 2012–2016. Neuro Oncol. 2019;21(Suppl 5):v1–100. https://doi.org/10.1093/neuonc/noz150.
27. Wee P, Wang Z. Epidermal Growth Factor Receptor cell proliferation signaling pathways. Cancers (Basel). 2017. https://doi.org/10.3390/cancers9050052.
28. Bahar ME, Kim HJ, Kim DR. Targeting the RAS/RAF/MAPK pathway for cancer therapy: from mechanism to clinical studies. Signal Transduct Target Ther. 2023;8(1):455. https://doi.org/10.1038/s41392-023-01705-z.
29. de Los Reyes Corrales T, Losada-Pérez M, Casas-Tintó S. JNK pathway in CNS pathologies. Int J Mol Sci. 2021. https://doi.org/10.3390/ijms22083883.
30. Wagner EF, Nebreda AR. Signal integration by JNK and p38 MAPK pathways in cancer development. Nat Rev Cancer. 2009;9(8):537–49. https://doi.org/10.1038/nrc2694.
31. Iyer VJ, Donahue JE, Osman MA. Role of scaffold proteins in the heterogeneity of glioblastoma. Cell Commun Signal. 2024;22(1):477. https://doi.org/10.1186/s12964-024-01809-1.
32. Fangusaro J, Jones DT, Packer RJ, Gutmann DH, Milde T, Witt O, et al. Pediatric low-grade glioma: state-of-the-art and ongoing challenges. Neuro Oncol. 2024;26(1):25–37. https://doi.org/10.1093/neuonc/noad195.
33. O'Hare P, Cooney T, de Blank P, Gutmann DH, Kieran M, Milde T, et al. Resistance, rebound, and recurrence regrowth patterns in pediatric low-grade glioma treated by MAPK inhibition: a modified Delphi approach to build international consensus-based definitions-International Pediatric Low-Grade Glioma Coalition. Neuro Oncol. 2024;26(8):1357–66. https://doi.org/10.1093/neuonc/noae074.
34. Biau J, Thivat E, Chautard E, Stefan D, Boone M, Chauffert B, et al. Phase 1 trial of ralimetinib (LY2228820) with radiotherapy plus concomitant temozolomide in the treatment of newly diagnosed glioblastoma. Radiother Oncol. 2021;154:227–34. https://doi.org/10.1016/j.radonc.2020.09.036.
35. Wang Q, Du J, Xu B, Xu L, Wang X, Liu J, et al. Silence of bFGF enhances chemosensitivity of glioma cells to temozolomide through the MAPK signal pathway. Acta Biochim Biophys Sin. 2016;48(6):501–8. https://doi.org/10.1093/abbs/gmw035.
36. Nicholson JG, Fine HA. Diffuse glioma heterogeneity and its therapeutic implications. Cancer Discov. 2021;11(3):575–90. https://doi.org/10.1158/2159-8290.Cd-20-1474.
37. Mohile NA, Messersmith H, Gatson NT, Hottinger AF, Lassman A, Morton J, et al. Therapy for diffuse astrocytic and oligodendroglial tumors in adults: ASCO-SNO guideline. J Clin Oncol. 2022;40(4):403–26. https://doi.org/10.1200/jco.21.02036.
38. Zhang Y, Gao X, Yi J, Sang X, Dai Z, Tao Z, et al. BTF3 confers oncogenic activity in prostate cancer through transcriptional upregulation of Replication Factor C. Cell Death Dis. 2021;12(1):12. https://doi.org/10.1038/s41419-020-03348-2.
39. Ke X, Li K, Jiang A, Zhang Y, Wang Q, Li Z, et al. Cloud-based GWAS platform: an innovative solution for efficient acquisition and analysis of genomic data. Med Res. 2025;1(3):397–411. https://doi.org/10.1002/mdr2.70040.
40. Gong Z, Du M, Li Y, Ye B, Huang Y, Gong H, et al. Machine learning identifies TIME subtypes linking EGFR mutations and immune states in lung adenocarcinoma. NPJ Digit Med. 2025;8(1):796. https://doi.org/10.1038/s41746-025-02172-2.
41. Zhang P, Liang X, Ye B, Wang X, Wang Y, Gong Z, et al. Metabolic reprogramming signature predicts immunotherapy efficacy in lung adenocarcinoma: targeting SLC25A1 to overcome immune resistance. Chin J Cancer Res. 2025;37(6):1000–19. https://doi.org/10.21147/j.issn.1000-9604.2025.06.11.
42. Xia L, Oyang L, Lin J, Tan S, Han Y, Wu N, et al. The cancer metabolic reprogramming and immune response. Mol Cancer. 2021;20(1):28. https://doi.org/10.1186/s12943-021-01316-8.
43. Faubert B, Solmonson A, DeBerardinis RJ. Metabolic reprogramming and cancer progression. Science. 2020. https://doi.org/10.1126/science.aaw5473.
44. Vander Heiden MG, Cantley LC, Thompson CB. Understanding the Warburg effect: the metabolic requirements of cell proliferation. Science. 2009;324(5930):1029–33. https://doi.org/10.1126/science.1160809.
45. Papsdorf K, Miklas JW, Hosseini A, Cabruja M, Morrow CS, Savini M, et al. Lipid droplets and peroxisomes are co-regulated to drive lifespan extension in response to mono-unsaturated fatty acids. Nat Cell Biol. 2023;25(5):672–84. https://doi.org/10.1038/s41556-023-01136-6.
46. Guo Z, Bergeron KF, Lingrand M, Mounier C. Unveiling the MUFA-cancer connection: insights from endogenous and exogenous perspectives. Int J Mol Sci. 2023. https://doi.org/10.3390/ijms24129921.
47. Maliekal P, Sokolova T, Vertommen D, Veiga-da-Cunha M, Van Schaftingen E. Molecular identification of mammalian phosphopentomutase and glucose-1,6-bisphosphate synthase, two members of the alpha-D-phosphohexomutase family. J Biol Chem. 2007;282(44):31844–51. https://doi.org/10.1074/jbc.M706818200.
48. Safari MS, Woerl P, Garmsiri C, Weber D, Kwiatkowski M, Hotze M, et al. Glucose-1,6-bisphosphate: a new gatekeeper of cerebral mitochondrial pyruvate uptake. Mol Metab. 2024;88:102018. https://doi.org/10.1016/j.molmet.2024.102018.
49. Qin W, Chen B, Li X, Zhao W, Wang L, Zhang N, et al. Cancer-associated fibroblasts secrete CSF3 to promote TNBC progression via enhancing PGM2L1-dependent glycolysis reprogramming. Cell Death Dis. 2025;16(1):249. https://doi.org/10.1038/s41419-025-07580-6.
50. Han ZG, Zhang QH, Ye M, Kan LX, Gu BW, He KL, et al. Molecular cloning of six novel Krüppel-like zinc finger genes from hematopoietic cells and identification of a novel transregulatory domain KRNB. J Biol Chem. 1999;274(50):35741–8. https://doi.org/10.1074/jbc.274.50.35741.
51. Harper J, Yan L, Loureiro RM, Wu I, Fang J, D'Amore PA, et al. Repression of vascular endothelial growth factor expression by the zinc finger transcription factor ZNF24. Cancer Res. 2007;67(18):8736–41. https://doi.org/10.1158/0008-5472.Can-07-1617.
52. Li W, Han S, Hu P, Chen D, Zeng Z, Hu Y, et al. LncRNA ZNFTR functions as an inhibitor in pancreatic cancer by modulating ATF3/ZNF24/VEGFA pathway. Cell Death Dis. 2021;12(9):830. https://doi.org/10.1038/s41419-021-04119-3.
53. Wen T, Zhang X, Gao Y, Tian H, Fan L, Yang P. SOX4-BMI1 axis promotes non-small cell lung cancer progression and facilitates angiogenesis by suppressing ZNF24. Cell Death Dis. 2024;15(9):698. https://doi.org/10.1038/s41419-024-07075-w.
54. Liu L, Lei Y, Chen W, Zhou Q, Zheng Z, Zeng G, et al. In vivo genome-wide CRISPR screening identifies ZNF24 as a negative NF-κB modulator in lung cancer. Cell Biosci. 2022;12(1):193. https://doi.org/10.1186/s13578-022-00933-0.
55. Niu L, Thiele M, Geyer PE, Rasmussen DN, Webel HE, Santos A, et al. Non-invasive proteomic biomarkers for alcohol-related liver disease. Nat Med. 2022;28(6):1277–87. https://doi.org/10.1038/s41591-022-01850-y.
56. Sherman BT, Hao M, Qiu J, Jiao X, Baseler MW, Lane HC, et al. DAVID: a web server for functional enrichment analysis and functional annotation of gene lists (2021 update). Nucleic Acids Res. 2022;50(W1):W216–21. https://doi.org/10.1093/nar/gkac194.
57. Subramanian A, Tamayo P, Mootha VK, Mukherjee S, Ebert BL, Gillette MA, et al. Gene set enrichment analysis: a knowledge-based approach for interpreting genome-wide expression profiles. Proc Natl Acad Sci U S A. 2005;102(43):15545–50. https://doi.org/10.1073/pnas.0506580102.
58. Shen W, Song Z, Zhong X, Huang M, Shen D, Gao P, et al. Sangerbox: a comprehensive, interaction-friendly clinical bioinformatics analysis platform. Imeta. 2022;1(3):e36. https://doi.org/10.1002/imt2.36.

Publisher's Note